LUNAR INTERIOR STUDIES USING LUNAR PROSPECTOR LINE-OF-SIGHT ACCELERATION DATA. T. Sugano, *Graduate University for Advanced Studies, 2-12 Hoshigaoka Mizusawa Iwate 023-0861, Japan (sugano@miz.nao.ac.jp)*, K. Heki, *National Astronomical Observatory, 2-12 Hoshigaoka Mizusawa Iwate 023-0861, Japan (heki@miz.nao.ac.jp)*.

Introduction : Gravity field studies have been playing an important role in investigating physical properties, origin, and evolution of terrestrial planets and satellites. Information on the lunar gravity field has been provided by radio tracking data of lunar satellites. Several gravity field models, based on a spherical harmonic expansion, have been produced from the analysis of these tracking data. Recent two lunar satellites, the Clementine [1] and the Lunar Prospector (LP) in 1990's, dramatically improved the accuracy of the gravity field model. Among them, the LP was launched on January 7, 1998 [2]. After finishing the 1 year nominal mission at the 100 km altitude polar orbit, 6-months long extended mission was carried at the average height of 30 km. The highest-resolution gravity model called LP165P was produced from the low-altitude extended mission tracking data [3]. Lunar gravity studies have a difficulty peculiar to the Moon, i.e., direct tracking data are available only at the lunar nearside because of synchronized spin and orbital motion of the Moon. The lack of farside data has been hindering us from making high-resolution gravity anomaly map. The LP165P gravity anomaly map, obtained imposing artificial constraints to stabilize the estimation of spherical harmonic coefficients using only nearside tracking data. As a result the LP165P has many spurious linear features; the model is reliable only up to 110th degree/order at the nearside and 60th degree/order at the farside [3].

Free-air anomaly map from the LP LOS data : Alternatively, line-of-sight (LOS) acceleration data of the LP satellite during its extended low-altitude mission are opened to the public at the Planetary Data System Geosciences Node web site (http://wwwpds.wustl.edu). Direct inversion of such data into surface mass distribution has several merits, e.g., high resolution can be attained without relying on artificial constraints, and short computation time by estimating regional parameter sets stepwise etc. We downloaded the LOS data product and used them for making free-air gravity anomaly map [4]. The bulk of lunar gravity fields can be approximated by those due to a point mass at the lunar center-of-mass, which we call the "reference field". We assume that excess masses (or mass deficits), responsible for the anomalous gravity, are condensed in a thin layer on the reference surface (a sphere with a radius $1,738$ km). We divide the lunar surface into $20^\circ \times 20^\circ$ "large blocks" (about 600 km $\times$ 600 km). They are subdivided into $0.8^\circ \times 0.8^\circ$ "small blocks" (about 25 km $\times$ 25 km). The "large block" is a unit of least-square estimation runs, and the "small block" corresponds to a parameter (mass) to be estimated. Assuming an anomalous gravity fields at satellite positions are sum of the gravitational pulls of individual small blocks, we estimate their masses so that they explain the observed LOS acceleration best in a least-squares sense. The LOS direction changes in time due to optical libration of the Moon is taken into account. The estimated surface masses are easily converted into free-air gravity anomaly (i.e., gravity anomaly at reference surface) by multiplying $2\pi G$, where G is the universal gravitational constant [5]. Resolution of the free-air anomaly map is $0.8^\circ \times 0.8^\circ$ (about 24 km $\times$ 24 km at lunar surface), equivalent to conventional model using spherical harmonics complete to 225th degree/order with less spurious signatures than past models (Fig. 1a).

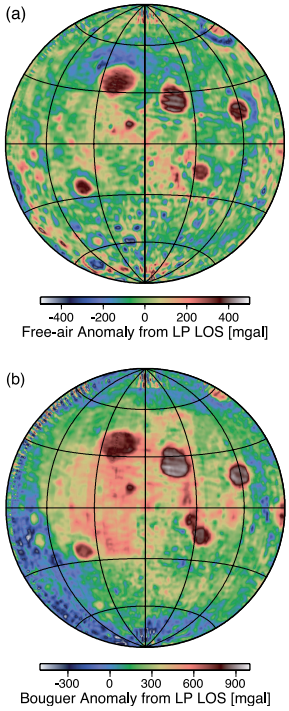

Figure 1: (a) Free-air gravity anomaly map obtained from direct inversion of LP LOS ata, and (b) Bouguer anomaly map using LP LOS data and Clementine grid topography data with assuming crustal density of $2,900$ kg m^{-3}. Gravity arises from mare basalt at mascon basins are corrected.

Terrain correction for the LP LOS data – Bouguer anomaly map : We perform terrain corrections for the raw LOS acceleration data using lunar topography data obtained by the Clementine laser altimetry. We calculate gravitational acceleration at a satellite positions due to the excess mass or mass deficit at each grid point given by the topography model. They are integrated over entire of the Moon, and projected into LOS direction. Such topographic contributions are subtracted from individual raw LOS accelerations. This terrain-corrected LOS data are processed in the same procedure as obtaining free-air anomaly map [4]. Although the derivation method is somewhat different from Earth's case, the obtained gravity anomaly corresponds to what we call "Bouguer anomaly", i.e., the gravity anomaly mainly reflecting the Moho topogra-

phy. As a special occasion for the Moon, gravity contributions arise from the excess mass of mare basalt are subtracted from the Bouguer anomaly in order to isolate gravity signals of the Moho topography at mascon basin [6, 7, 8]. The Bouguer anomaly map is useful to study deep interiors since it is supposed to be free from gravity signals of the surface topography. The obtained Bouguer anomaly map is shown in Fig. 1b.

Mass deficits from the gravity anomaly maps : We estimate mass deficits associated with the 92 of medium-sized craters (about 60 – 160 km diameter) from Bouguer anomaly map for the purpose of studying their compensation states. To obtain mass deficit of a crater, we follow steps, (1) define a circle which is larger than crater rim, (2) background values of the Bouguer gravity anomaly are obtained as their average over the circle, (3) surface mass density relative to the background values are integrated over the interior of the circle. Figure 2a shows that the mass deficits are almost zero for the medium-sized craters. This suggests the Moho topographies beneath them are flat, i.e., no compensation occurred for these medium-sized craters.

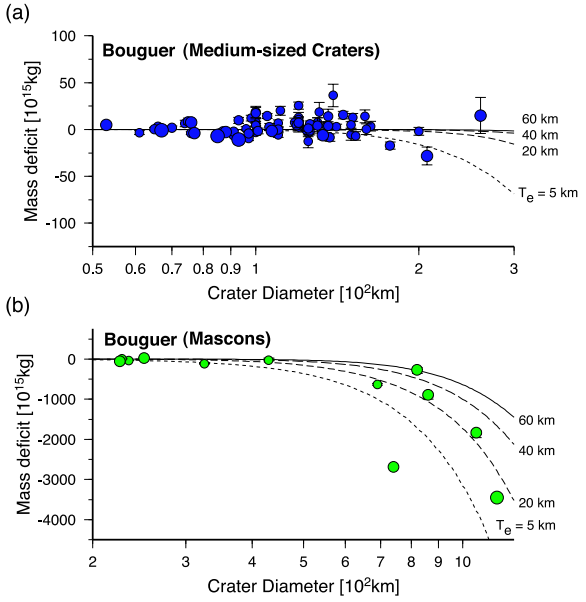

Figure 2: Mass deficits associate with 92 of medium-sized craters (a) and 12 of mascons (b) from Bouguer anomaly map. The curves denote mass deficits inferred from Moho topography model with elastic thickness $T_e = 5$, 20, 40, 60 km.

In addition to the medium-sized craters, we evaluate mass deficits for mascons (about 200 – $1,100$ km diameter). We estimate elastic thickness (or thickness of lithosphere; T_e) beneath the mascons from Moho topography inferred from mass deficit. The results indicate lunar lithosphere was as thick as 20 – 60 km at the time of the mascon formation (Fig. 2b). The elastic thickness beneath mascons are highly depend on the location, rather than the age. Mascons larger than 400 km diameter is categorized into three group based on their elastic thickness (Fig. 3). Location of the mascons belong to same group are neighboring each other. Head and Wilson (1992) pointed out that the nearside-farside variation in crustal thickness was established, perhaps by convection associated with the magma ocean or by the formation of the Procellarum basin during Pre-Nectarian period, and this initial difference in crustal thickness had a major influence on the subsequent emplacement of mare basalts and compensation state of craters. If we adopt the hypothetical Procellarum basin, these mascon groups are located at (A) inside, (B) south-eastern edge, and (C) south-western edge of the basin, respectively (Fig. 3). Center of the Procellarum basin is thought to be located at 23°N, 15°W, near the crater Timocharis, and diameter of the largest concentric ring is $3,200$ km [10]. Imbrium and Serenitatis basin are located near a center of the Procellarum basin. They represent anomalously thin lithosphere. In addition, several volcanic origin mascons are found at inside of the Procellarum basin. Perhaps the presence of the Procellarum basin may be exerting an influence in terms of relatively thin crust and lithosphere in this region. Although Group C is closer to the center of Procellarum basin than Group B, the elastic thickness is thicker than Group B. Western part of Procellarum basin tend to possess thicker lithosphere.

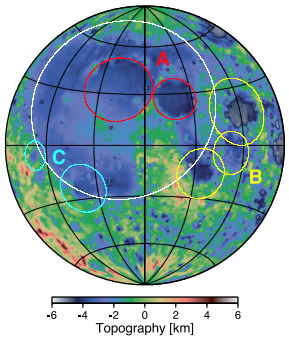

Figure 3: Distribution of mascon groups and Procellarum basin on topography map from the Clementine. White circle denotes largest ring of Procellarum basin. Colored circles are mascons with $T_e < 10$ km (Group A, red), ~ 30 km (Group B, yellow), and 60 km (Group C, light-blue).

References : [1] Nozette, S., et al. (1994) *Science*, *266*, 1835–+. [2] Binder, A. B. (1998) *Science*, *281*, 1475–1476. [3] Konopliv, A. S., S. W. Asmar, E. Carranza, W. L. Sjogren, and D. N. Yuan (2001) *Icarus*, *150*, 1–18. [4] Sugano, T., and K. Heki (2004) *Earth Planets and Space*, in press. [5] Garland, G. D. (1965) Pergamon Press. [6] Parker, R. L. (1972) *J. R. Astron. Soc.*, *31*, 447–455. [7] Williams, K. K., and M. T. Zuber (1996) in *Lunar and Planetary Institute Conference Abstracts*, pp. 1441–1442. [8] Solomon, S. C., and J. W. Head (1980) *Reviews of Geophysics and Space Physics*, *18*, 107–141. [9] Head, J. W., and L. Wilson (1992) *Geochim. Cosmochim. Acta*, *56*, 2155–2175. [10] Whitaker, E. A. (1981) in *Multi-ring basins: Formation and Evolution*, pp. 105–111.